Formation of Molecular-Orbital Bands in a Twisted Hubbard Tube: Implications for Unconventional Superconductivity in $K_2Cr_3As_3$

Hanting Zhong,[1] Xiao-Yong Feng,[1,2,*] Hua Chen,[3,4] and Jianhui Dai[1,2,†]
[1]Condensed Matter Group, Department of Physics, Hangzhou Normal University, Hangzhou 310036, China
[2]Hangzhou Key Laboratory of Quantum Matter, Hangzhou Normal University, Hangzhou 310036, China
[3]International Center for Quantum Materials and School of Physics, Peking University, Beijing 100871, China
[4]Collaborative Innovation Center of Quantum Matter, Beijing 100871, China
(Received 5 April 2015; revised manuscript received 21 June 2015; published 24 November 2015)

We study a twisted Hubbard tube modeling the $[CrAs]_\infty$ structure of quasi-one-dimensional superconductors $A_2Cr_3As_3$ (A = K, Rb, Cs). The molecular-orbital bands emerging from the quasi-degenerate atomic orbitals are exactly solved. An effective Hamiltonian is derived for a region where three partially filled bands intersect the Fermi energy. The deduced local interactions among these active bands show a significant reduction compared to the original atomic interactions. The resulting three-channel Luttinger liquid shows various interaction-induced instabilities including two kinds of spin-triplet superconducting instabilities due to gapless spin excitations, with one of them being superseded by the spin-density-wave phase in the intermediate Hund's coupling regime. The implications of these results for the alkali chromium arsenides are discussed.

DOI: 10.1103/PhysRevLett.115.227001 PACS numbers: 74.20.Mn, 71.15.Mb, 74.70.-b, 74.78.Na

Introduction.—Recently, the alkali chromium arsenides $A_2Cr_3As_3$ (A = K, Rb, Cs) have been found as a new family of inorganic quasi-one-dimensional (Q1D) superconductors with strong electron correlations [1–3]. The basic building block of these compounds is the $[CrAs]_6$ cluster consisting of two conjugated triangular complexes $[CrAs]_3$ as shown schematically in Fig. 1(a). They are aligned along the c axis forming a $[CrAs]_\infty$ tube, and intercalated by A^+ cations forming a hexagonal lattice. The density functional theory (DFT) calculations [4,5] predict a three-dimensional (3D) Fermi surface (FS) sheet (γ band) and two Q1D FS sheets (α and β bands), essentially due to the Cr $3d$ electrons. The NMR experiment [6] has revealed a power law behavior of the spin-lattice relaxation rate, manifesting the Luttinger liquid feature above T_c. The penetration depth measurement [7] has evidenced a line nodal feature in the pairing state below T_c.

Because of the existing 3D γ band, whether the superconductivity solely originates from the Q1D structure of $A_2Cr_3As_3$ is uncertain. In fact the nearly isotropic 3D bulk CrAs compound shows superconductivity with $T_c \sim 2.2$ K under pressure of ~0.7 GPa [8,9]. Interestingly, Zhou *et al.* pointed out that an f-wave pairing state could arise from the 3D band with a node line while a fully gapped p-wave pairing state could dominate at the Q1D band [10]. Such triplet superconductivity, with some variations in spatial symmetry [11], could be driven by ferromagnetic fluctuations within the sublattice of Cr atoms [4,11].

In order to understand the formation of the low energy bands, it is particularly important to understand the electronic property of *a single fundamental* $[CrAs]_\infty$ *tube*. In this Letter, we model this system by a twisted Hubbard lattice composed of triangular complexes coupled along the c axis with the glide reflection symmetry as shown in Fig. 1(b) [12]. In each unit cell there are six Cr atoms, each with five $3d$ atomic orbitals (AOs). The influence of the As $4p$ orbitals can be effectively accounted for by the indirect hopping of Cr-$3d$ electrons. So the model involves thirty energy bands in total. In the realistic case, fortunately, only three partially filled bands are active in the low energy regime. We will explicitly show how these bands come from the molecular orbitals (MOs) of $[CrAs]_6$ [4,10]. Our purpose is then to understand their cooperative low temperature physics within the Luttinger liquid approach. The proposed effective model is of interest in its own right as we shall explore in the following.

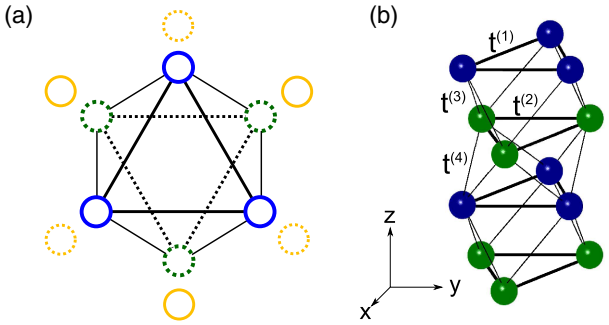

FIG. 1 (color online). (a) A CrAs cluster in the *ab* plane. The solid (dotted) circles connected by the solid (dotted) lines represent the Cr atoms in the first (second) triangle in a unit cell. The isolated outer solid (dotted) circles represent the As atoms in the corresponding planes. (b) A Q1D CrAs tube. The blue (green) filled circles represent the Cr atoms in each triangles. The As atoms are not shown.

Model hamiltonian.—The Hubbard model for a single $[\mathrm{CrAs}]_\infty$ tube is expressed as $H = H_0 + H_{\mathrm{int}}$, where, H_0 represents the noninteracting part consisting of the tight-binding kinetic energy and the crystalline electric field (CEF) splitting,

$$H_0 = -\sum_{\mathbf{r}\mathbf{r}'mm'\sigma} t_{mm'}^{(\mathbf{r},\mathbf{r}')} d_{\mathbf{r}\sigma}^{\dagger(m)} d_{\mathbf{r}'\sigma}^{(m')} + \sum_{\mathbf{r}m\sigma} E_{\mathbf{r}m} n_{\mathbf{r}\sigma}^{(m)}. \quad (1)$$

Here, $d_{\mathbf{r}\sigma}^{(m)}$ denotes the annihilation operator of Cr $3d$ electrons at the site $\mathbf{r}$ with angular momentum $m = 0$, ±1, ±2, spin $\sigma = \uparrow, \downarrow$. $n_{\mathbf{r}\sigma}^{(m)}$ and $\mathbf{S}_{\mathbf{r}}^{(m)}$ are the corresponding density and spin operators. The two twisted Cr triangles could have different $E_{\mathbf{r}m} = E_m^{(1)}$, $E_m^{(2)}$, accountable for the possible occupation difference [5], while

$$\begin{aligned} H_{\mathrm{int}} = {} & U\sum_{\mathbf{r}m} n_{\mathbf{r}\uparrow}^{(m)} n_{\mathbf{r}\downarrow}^{(m)} + \frac{2U' - J_H}{4} \sum_{\mathbf{r}m\neq m'\sigma\sigma'} n_{\mathbf{r}\sigma}^{(m)} n_{\mathbf{r}\sigma'}^{(m')} \\ & - J_H \sum_{\mathbf{r}m\neq m'} \mathbf{S}_{\mathbf{r}}^{(m)} \cdot \mathbf{S}_{\mathbf{r}}^{(m')} \\ & + J_p \sum_{\mathbf{r}m\neq m'} d_{\mathbf{r}\uparrow}^{\dagger(m)} d_{\mathbf{r}\downarrow}^{\dagger(m)} d_{\mathbf{r}\downarrow}^{(m')} d_{\mathbf{r}\uparrow}^{(m')} \end{aligned} \quad (2)$$

represents the local interactions including the intraorbital Coulomb interaction U, the interorbital Coulomb interaction U', the Hund's coupling J_H, and the pair-hopping J_p, respectively.

There are four kinds of adjacent intraorbital hoppings $t_{mm}^{(i)} \equiv t_m^{(i)}$ ($i = 1$–4), corresponding to the nearest-neighbor (NN) sites in the first and second triangles, and those between the intracell and intercell triangles, respectively, as illustrated in Fig. 1(b). Because of the metallic bonding among Cr atoms, the direct orbital mixings are relatively small, and the indirect hybridization is mainly bridged by the As $4p$ orbitals. So it is legitimate to consider a simpler situation for the adjacent interorbital hopping: $t_{mm'}^{(i)} = \eta t_m^{(i)} \delta_{|m|,|m'|}$ for $m \neq m'$, with $|\eta| < 1$. In this situation, the atomic orbitals are quasidegenerate as the nonvanishing mix terms are isotropic in space [13]. Finally, we include the next NN intraorbital hopping $t_m^{(5)}$ along the tube direction.

Molecular-orbital bands.—Denoting each site by $\mathbf{r} = (n, a, \xi)$, with $a = 1$, 2, 3 being the location in the first ($\xi = 1$) or second ($\xi = 2$) triangles in the nth unit cell, it is convenient to introduce a base $d_n^{(m)} = (d_{(n,1,1)}^{(m)}, d_{(n,1,2)}^{(m)}, d_{(n,2,1)}^{(m)}, d_{(n,2,2)}^{(m)}, d_{(n,3,1)}^{(m)}, d_{(n,3,2)}^{(m)})^T$ for the atomic m-orbital in the nth unit cell (the spin index σ is implied). For $m = 0$, this base accommodates a representation for the C_3 rotational symmetry, leading to six MOs corresponding to E, E', A, and A' states, respectively [14]. For $m = \pm1$ or ±2, we need to introduce a set of new bases $\tilde{d}_n^{(\pm|m|)} = (1/\sqrt{2})[d_n^{(m)} \pm d_n^{(-m)}]$. Thus for a single $[\mathrm{CrAs}]_6$ cluster, we have thirty MOs defined by $C_n^{(\tau)} = (\hat{R} \otimes \hat{Q}_0)\tilde{d}_n^{(\tau)}$ for $\tau = 0$ (denoting $\tilde{d}_n^{(0)} \equiv d_n^{(0)}$), ±1 and ±2, respectively, with ($\omega = e^{i\varphi}$, $\varphi = 2\pi/3$)

$$\hat{R} = \frac{1}{\sqrt{3}} \begin{pmatrix} 1 & 1 & 1 \\ 1 & \omega & \omega^{-1} \\ 1 & \omega^{-1} & \omega \end{pmatrix}, \quad \hat{Q}_0 = \frac{1}{\sqrt{2}} \begin{pmatrix} 1 & -1 \\ 1 & 1 \end{pmatrix}. \quad (3)$$

Note that the eigenstates of $\hat{R}$ with eigenvalues $\lambda_1 = 2$ and $\lambda_2 = \lambda_3 = -1$ correspond to the representations A and E, respectively.

When the triangles are coupled along the c axis via the intercell hopping $t_{mm'}^{(4)}$, we can extend $\hat{Q}_0$ to the momentum k-resolved matrix $\hat{Q}_a^{(\tau)}(k)$ so that the Bloch form $C_k^{(\tau)} = (c_{(k,1,1)}^{(\tau)}, c_{(k,1,2)}^{(\tau)}, c_{(k,2,1)}^{(\tau)}, c_{(k,2,2)}^{(\tau)}, c_{(k,3,1)}^{(\tau)}, c_{(k,3,2)}^{(\tau)})^T$ is still a natural base diagonalizing H_0, leading to thirty MO bands labeled by the eigenenergies $\mathcal{E}_{(a,\xi)}^{(\tau)}(k)$. Here the subscript $\xi = 1$, 2 corresponds to the antibonding or bonding bands, respectively, due to the twisted structure. The explicit expressions of $\hat{Q}_a^{(\tau)}(k)$ and $\mathcal{E}_{(a,\xi)}^{(\tau)}(k)$, which also depend on the orbitals $\tau(= 0, \pm1, \pm2)$ and C_3 eigenvalues $\lambda_a (a = 1, 2, 3)$, are presented in the Supplemental Material (SM) [15]. A set of subscripts (a, ξ) determines the symmetry property of the corresponding MO bands.

We fitted the DFT band structure along the tube direction using the obtained MO bands within $\tau = 0$, ±2, while the bands with $\tau = \pm1$ are fairly away from the Fermi energy as revealed in the DFT calculations [4,5]. The three partially filled DFT bands, i.e., the 3D γ band characterized mainly by the d_{z^2} orbital ($m = 0$), the Q1D α and β bands characterized mainly by the d_{xy} and $d_{x^2-y^2}$ orbitals ($|m| = 2$), are all holelike near the Γ point ($k = 0$) and electronlike near the A point($k = \pi$). Therefore, the γ band corresponds to the singlet MO band labeled by ($\tau = 0$, $a = 1$, $\xi = 1$). The α and β bands, which are degenerate along the whole $\Gamma \to A$ direction, correspond to the doublet MO bands labeled by ($\tau = -2$, $a = 2$, $\xi = 2$) and ($\tau = -2$, $a = 3$, $\xi = 2$), respectively. The best fitting using $\mathcal{E}_{(1,1)}^{(0)}$, $\mathcal{E}_{(2,2)}^{(-2)} = \mathcal{E}_{(3,2)}^{(-2)}$ is shown in Fig. 2 [15]. Here, the tight-binding parameters are not uniquely determined because the number of these parameters exceeds eight necessary coefficients in the fitting. On the other hand, the precise values of the fitting parameters are not important in the present study. As we shall find later, only the symmetry property of the MO bands and local interactions between them play a crucial role in the Luttinger liquid approach.

For simplicity, from now on, we shall use the band subscript $\nu(= 1, 2, 3)$ to account for the three MO bands intersecting the Fermi energy. These active MO bands are associated with phases $\varphi_\nu = 0$, $2\pi/3$, $-2\pi/3$, or chiralities $\vartheta_\nu = 0$, 1, and -1, respectively. In the full 1D Brillouin zone, there are three pairs of Fermi points $(k_{F_\nu}, -k_{F_\nu})$, satisfying $0 < k_{F_1} < k_{F_2} = k_{F_3} < \pi$, as schematically

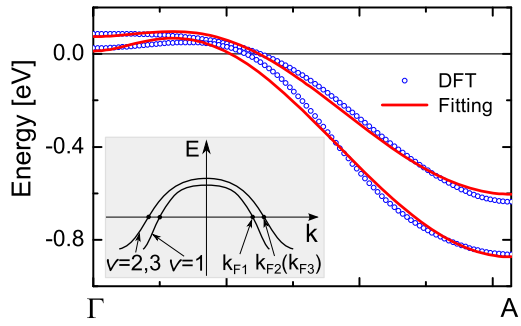

FIG. 2 (color online). Fitting the band structure: The upper band is twofold degenerate. The lower inset is the schematic picture for the three partially filled bands with three pairs of Fermi points.

shown in the inset of Fig. 2. By integrating out all inactive bands, we obtain the effective theory describing the low energy property of the active bands:

$$H_{\rm eff} = \sum_{k\nu_i\sigma} \mathcal{E}_\nu(k)\hat{n}_{k\nu\sigma} + \sum_n H_{\rm int}^{(n)}. \tag{4}$$

Where, $\hat{n}_{k\nu\sigma} = c^\dagger_{k\nu\sigma}c_{k\nu\sigma}$ is the density operator of electrons in the νth MO band, $H_{\rm int}^{(n)}$ the residual short-range interactions in the MOs in the nth unit cell, given by

$$\begin{aligned} H_{\rm int}^{(n)} = & \sum_\nu \tilde{U}_\nu \hat{n}_{\nu\uparrow}(n)\hat{n}_{\nu\downarrow}(n) + \sum_{\nu\neq\nu'\sigma\sigma'} \tilde{U}_{\nu\nu'}\hat{n}_{\nu\sigma}(n)\hat{n}_{\nu'\sigma'}(n) \\ & - \sum_{\nu\neq\nu'} \tilde{J}_{\nu\nu'}\hat{\mathbf{S}}_\nu(n)\cdot\hat{\mathbf{S}}_{\nu'}(n) \\ & + \tilde{J}_{123}[c^\dagger_{1\uparrow}(n)c^\dagger_{1\downarrow}(n)c_{2\downarrow}(n)c_{3\uparrow}(n) + (2\leftrightarrow 3) + \text{H.c.}]. \end{aligned} \tag{5}$$

In this expression, the electron annihilation operator in the nth unit cell is defined by the Fourier transformation $c_{\nu\sigma}(n) = (1/\sqrt{2\pi})\sum_k e^{iknc_0}c_{k\nu\sigma}$ (with c_0 the lattice spacing taken as unit). Only those terms preserving the neutrality condition $\sum_{\nu_i}\vartheta_{\nu_i} = 0$ could survive. The matrix $\hat{Q}_0$ is used in deducing Eq. (5) as the short-range interactions are mainly due to the slowly varying part, leading to $\tilde{U}_1 = U/6$, $\tilde{U}_2 = \tilde{U}_3 = (U + U' + J_H + J_p)/12$; $\tilde{U}_{12} = \tilde{U}_{13} = U'/12 - J_H/24$; $\tilde{U}_{23} = (U + U' + J_H + J_p)/48$; $\tilde{J}_{12} = \tilde{J}_{13} = J_H/6$; $\tilde{J}_{23} = (U + U' + J_H + J_p)/12$; and $\tilde{J}_{123} = J_p/6$. The influence of inactive bands is mainly attributed to the renormalized tight-binding parameters.

The luttinger liquid in the weak-coupling regime.—We now take the continuous limit, linearize the active bands near the Fermi points, and decompose the electron operator into right and left moving components like $c_{\nu\sigma}(z) \approx e^{-ik_{F_\nu}z - i\varphi_\nu}L_{\nu\sigma}(z) + e^{+ik_{F_\nu}z + i\varphi_\nu}R_{\nu\sigma}(z)$. Here, $z = nc_0$ is the spatial coordinate along the tube direction, $R_{\nu\sigma}$ and $L_{\nu\sigma}$ represent the right and left moving fermions describing the low energy excitations near the Fermi points $(k_{F_\nu}, -k_{F_\nu})$ with linear dispersion $\pm v_{F_\nu}k$. The long-wavelength, low-energy effective Hamiltonian (density) is given by $\mathcal{H}_{\rm eff} = \mathcal{H}_0 + \mathcal{H}_{\rm int}$, where $\mathcal{H}_0 = \sum_{\nu,\sigma}(iv_{F_\nu})[R^\dagger_{\nu\sigma}\partial_z R_{\nu\sigma} - L^\dagger_{\nu\sigma}\partial_z L_{\nu\sigma}]$ is the kinetic part, and $\mathcal{H}_{\rm int}$ includes various residual interactions which are usually expressed in terms of the g-ology [16,17]. We shall assume the Fermi velocities v_{F_ν} to be the same as this does not influence the nature of superconductivity we are concerned with. The corresponding one-loop renormalization group (RG) equations resemble those for three-leg Hubbard ladders [18,19] or a variant of carbon nanotubes [20–22]. The instabilities of these RG equations are classified routinely: (i) the intraband instabilities as those developed in the single-channel Luttinger liquid [23], and (ii) the interband instabilities as those developed in the two-channel band Luttinger liquid. Note that the three-band interaction in Eq. (5) does not lead to the peculiar three-band instability suggested in Ref. [22] as shown in the SM [15,24]. All these suggest the validity of the conventional bosonization approach based on spin-charge separation, where various ordering instabilities can be determined by Luttinger parameters. The new ingredients here are the peculiar symmetry surviving in the active MO bands and their dependence on local electron interactions.

The right- and left-moving fields are then expressed in terms of the charge fields $(\phi_{\nu,c}, \theta_{\nu,c})$ and the spin fields $(\phi_{\nu,s}, \theta_{\nu,s})$ (for each $\nu = 1, 2, 3$) by

$$\begin{aligned} R_{\nu,\sigma}(z) &= \frac{F_{R,\nu\sigma}}{\sqrt{2\pi c_0}} e^{i\sqrt{\pi/2}(\theta_{c,\nu} + \sigma\theta_{s,\nu} - \phi_{c,\nu} - \sigma\phi_{s,\nu})}, \\ L_{\nu,\sigma}(z) &= \frac{F_{L,\nu\sigma}}{\sqrt{2\pi c_0}} e^{i\sqrt{\pi/2}(\theta_{c,\nu} + \sigma\theta_{s,\nu} + \phi_{c,\nu} + \sigma\phi_{s,\nu})}. \end{aligned} \tag{6}$$

The Klein factors $F_{R,\nu\sigma}$ and $F_{L,\nu\sigma}$ ensure the fermionic statistics between the right and left moving fermions. Next, in order to diagonalize the kinetic part, we need to introduce a set of new bases

$$\begin{aligned} \tilde{\phi}_{\gamma,i} &= \eta_{\gamma,i}(q_{\gamma,i}\phi_{\gamma,1} + \phi_{\gamma,2} + \phi_{\gamma,3}), \\ \tilde{\phi}_{\gamma,3} &= \frac{1}{\sqrt{2}}(-\phi_{\gamma,2} + \phi_{\gamma,3}), \end{aligned} \tag{7}$$

where $\gamma = s,\ c$, $q_{\gamma,i} = -[b_\gamma + (-1)^i\sqrt{8a_\gamma^2 + b_\gamma^2}/2a_\gamma]$ for $i = 1, 2$, $a_c = (2\tilde{U}_{12}/\pi)$, $b_c = (2\tilde{U}_{23}/\pi)$, $a_s = -(\tilde{J}_{12}/2\pi)$, $b_s = -(\tilde{J}_{23}/2\pi)$, $\eta_{\gamma,i}$ are the normalization constants. Similar relationships apply to the fields $\theta_{\gamma,i}$ and $\tilde{\theta}_{\gamma,i}$ for $i = 1, 2, 3$. Hence, we arrive at the following three-channel Tomonaga-Luttinger liquid Hamiltonian:

$$\tilde{H}_0 = \int dz \sum_{i=1,2,3,\gamma=s,c} \left[\frac{v_F}{2}(\nabla\tilde{\theta}_{\gamma,i})^2 + \lambda_{\gamma,i}(\nabla\tilde{\phi}_{\gamma,i})^2\right] \tag{8}$$

where, $\lambda_{\gamma,i} = t_\gamma + \frac{1}{2}[b_\gamma - (-1)^i\sqrt{8a_\gamma^2 + b_\gamma^2}]$ for $i = 1, 2$, and $\lambda_{\gamma,3} = t_\gamma - b_\gamma$, $t_c = (v_F/2) + (\tilde{U}_1/2\pi)$, $t_s = (v_F/2) - (\tilde{U}_1/2\pi)$. Therefore, the Luttinger parameters are obtained explicitly by

$$K_{c,i} = \left[1 + \frac{U}{4\pi v_F} - \frac{(-1)^i}{12\pi v_F}\sqrt{8(2U - 5J_H)^2 + U^2}\right]^{-\frac{1}{2}},$$
$$K_{s,i} = \left[1 - \frac{U}{4\pi v_F} - \frac{(-1)^i}{12\pi v_F}\sqrt{8J_H^2 + U^2}\right]^{-\frac{1}{2}}$$

for the channels $i = 1, 2$, respectively, and $K_{c,3} = K_{s,3} = 1$ for the third channel $i = 3$. Here, we have adopted the conventional relations $J_p = J_H$ and $U' = U - 2J_H$, reflecting the rotational symmetry of the original AOs [25].

Now since $U > 0$ and $J_H > 0$, one can find that: (i) $K_{c,1} < 1$ in the entire region and $K_{s,1} < 1$ only when $U < J_H$; (ii) $K_{c,2} < 1$ in the region $0.2U < J_H < 0.6U$ and $K_{s,2} > 1$ in the entire region. Specifically, in the physically relevant regime, $U > J_H$, the spin excitations are always gapless, so $K_{s,i}$ could be fixed to the unit due to the spin-SU(2) symmetry. Because $K_{c,1} < 1$, the channel 1 is in the spin-density-wave (SDW) phase [16,17]. The channel 3 involves the antibonding of the MO bands $\nu = 2, 3$ as shown in Eq. (7). In this channel both spin and charge excitations are critical. Because of the absence of a spin gap, the dominating superconducting instability is the interband spin triplet pairing [16,17], driven by the interband scattering between the two Q1D α and β bands. The intriguing case is the channel 2, whose property depends on the ratio J_H/U. We plot in Fig. 3 the phase diagram determined by the Luttinger parameters in this channel. We find that $K_{c,2} > 1$ in the regimes separated by the orange-dotted and blue-dashed lines, respectively. In these two separated regimes, the dominating instability is still the spin-triplet pairing [16,17]. But in the intermediate regime where $K_{c,2} < 1$, the SDW instability dominates. It should be noticed that in either case where the interband triplet superconducting instabilities dominate, the spin-singlet superconducting instability is the subdominating instability [17,26].

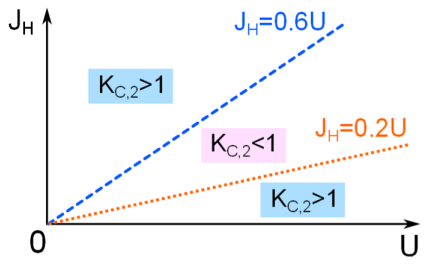

FIG. 3 (color online). Luttinger parameters for the channel 2: $K_{s,2} > 1$ everywhere, and $K_{c,2} < 1$ only in the intermediate regime between the lines $J_H = 0.2U$ and $J_H = 0.6U$.

In order to see whether the above Luttinger liquid results are robust against deviations from the atomic orbital rotational symmetry, we have also considered a small deviation ΔU away from the rotational symmetry by assuming $U' = U + \Delta U - 2J_H$. As shown in the SM, the channel 3 is still in the critical phase and the role of ΔU is to modify the value of U in a simple manner so that the results remain unchanged [15].

Summary and discussions.—We have focused on the microscopic formation of the MO bands in a twisted Hubbard tube capturing the Q1D nature of $K_2Cr_3As_3$, a new Q1D multiorbital superconducting molecular crystal with the moderate Coulomb interaction and Hund's coupling. A three-channel Tomonaga-Luttinger liquid Hamiltonian describing the low energy physics of the three active MO bands (the α, β, and γ bands) is then derived, showing possible unconventional triplet superconducting instabilities within a reasonable range of interaction parameters.

The conclusions and implications of our study are compared with the previous studies [10,11] where a phenomenological 3D Hubbard model for the three active MO bands was proposed based on the elegant symmetry argument [10] and investigated by the random phase approximation [10,11] and the mean field treatment [11]. First, the twisted structure of the Q1D $[CrAs]_\infty$ tube showing the extended glide reflection symmetry in accordance with the C_3 group is explored in our approach so that the symmetry property of all the thirty MO bands (including the three active MO bands) could be identified. Second, the interactions among the three active MO bands are derived from the microscopic atomic Hubbard interactions, different from those proposed phenomenologically. Third, the three diagonal channels in our Tomonaga-Luttinger Hamiltonian are superpositions of the original DFT bands, in contrast to the random phase approximation approach and the mean field treatment.

We found two kinds of spin-triplet pairing instabilities emerging out from two of the three channels. One involves the Q1D α and β bands, another involves all three bands. In the Luttinger liquid approach, triplet pairing instabilities are due to gapless spin excitations for $U > J_H$ and $K_c > 1$ in the corresponding channels. The ferromagnetic correlation within the sublattice of Cr atoms [4,11], though possible, is not a prerequisite of the triplet states. We also found an intermediate regime $0.2 < J_H/U < 0.6$ where the SDW phase emerges. Our solution is sensitive to the symmetry or regularity of the two conjugated Cr triangles, seemingly consistent with the recent hydrostatic and uniaxial pressure experimental study [27]. The exact mapping from the AOs to MO bands will also pave the way for further investigations on related effects such as the spin-orbit coupling within a microscopic framework.

As the present study is limited to the Q1D case, the spatial symmetry of the superconducting pairing states is not specified. However, the actual 3D superconductivity can

be perceived based on the Q1D physics because the identification of the three low energy MO bands is robust owing to the same symmetry argument. The local interactions among the MO bands are similar to those in the Q1D case. If the local atomic interactions are estimated as those in other Cr-based oxides, like $SrCrO_3$ [28], one has $U \sim 2.7 \pm 0.5$ eV, $J_H \sim 0.42 \pm 0.1$ eV, and $J_H/U \sim 0.16$, then in the Q1D case the channel 2 is in the triplet phase but close to the SDW low boundary $J_H/U = 0.2$ shown in Fig. 3. The corresponding residual MO interactions $\tilde{U}$ and $\tilde{J}$ in the 3D case are significantly suppressed, but the ratio $\tilde{J}/\tilde{U}$ enhanced [15], corresponding to the regime with small $\tilde{U}$ but relatively large $\tilde{J}/\tilde{U}$ in Ref. [10], where the triplet $f_{y(3x^2-y^2)}$ pairing state is favored. Of course, we have not considered the long-range Coulomb interaction and the electron-phonon coupling, the suppression of residual MO interactions should necessitate further investigations on these influences.

Finally, a more intriguing issue is the possible dimensional crossover from Q1D to 3D which could be tuned by either chemical substitution [2,3] or physical pressure [27,29]. On one hand, one of the three active bands, corresponding to $\nu = 1$, evolves with the intertube hopping and crossovers to the 3D γ band which could lead to the line nodal feature. Meanwhile, the (α, β) bands could remain Q1D because the intertube hopping among the AOs with $m = \pm 2$ is reasonably small. On the other hand, the Q1D superconducting instability can lead to a true long-range order when the intertube hopping is taken into account. Recall that the interband triplet pairing instability in the channel 2 is driven not only by the γ band, but also by the (α, β) bands. Consequently, the spin-triplet pairing instability in the channel 2 involves both the 3D and Q1D bands. As such a 3D pairing state could emerge from a normal state of an essentially Q1D Luttinger liquid characteristic, a scenario which is likely consistent with available experiments. It is desirable to investigate the related crossover behavior in this class of materials in the future.

We are grateful to Chao Cao, Guanghan Cao, and Yi Zhou for stimulating discussions. This work was supported in part by the NSF of China (under Grants No. 11274084, No. 11304071, and No. 11474082).

*fxyong@163.com
†daijh@zju.edu.cn

[1] J.-K. Bao *et al.*, Phys. Rev. X **5**, 011013 (2015).
[2] Z.-T. Tang, J.-K. Bao, Y. Liu, Y.-L. Sun, A. Ablimit, H.-F. Zhai, H. Jiang, C.-M. Feng, Z.-A. Xu, and G.-H. Cao, Phys. Rev. B **91**, 020506(R) (2015).
[3] Z.-T. Tang, J.-K. Bao, Z. Wang, H. Bai, H. Jiang, Y. Liu, H.-F. Zhai, C.-M. Feng, Z.-A. Xu, and G.-H. Cao, Sci. China Mater. **58**, 16 (2015).
[4] H. Jiang, G. Cao, and C. Cao, Sci. Rep. **5**, 16054 (2015).
[5] X. Wu, C.-C. Le, J. Yuan, H. Fan, and J.-P. Hu, Chin. Phys. Lett. **32**, 057401 (2015).
[6] H. Z. Zhi, T. Imai, F. L. Ning, J.-K. Bao, and G.-H. Cao, Phys. Rev. Lett. **114**, 147004 (2015).
[7] G. M. Pang, M. Smidman, W. B. Jiang, J. K. Bao, Z. F. Weng, Y. F. Wang, L. Jiao, J. L. Zhang, G. H. Cao, and H. Q. Yuan, Phys. Rev. B **91**, 220502(R) (2015).
[8] W. Wei, J. Cheng, K. Matsubayashi, P. Kong, F. Lin, C. Jin, N. Wang, Y. Uwatoko, and J. Luo, Nat. Commun. **5**, 5508 (2014).
[9] H. Kotegawa, N. Nakahara, H. Tou, and H. Sugawara, J. Phys. Soc. Jpn. **83**, 093702 (2014).
[10] Y. Zhou, C. Cao, and F. C. Zhang, arXiv:1502.03928.
[11] X. Wu, F. Yang, C. Le, H. Fan, and J. Hu, Phys. Rev. B **92**, 104511 (2015).
[12] The glide reflection symmetry is exact when the two conjugated triangles are equivalent and the corresponding hopping parameters and the CEF splittings in the Hamiltonian Eq. (1) are the same.
[13] The assumption of quasidegenerate AOs leads to a fixed AO content of each MO band along the $\Gamma \to A$ direction up to a rotation around the z axis. The variation of the AO contents does not alter the symmetry property and local interactions of the MOs.
[14] R. B. Tao, *Group Theory in Physics* (Higher Education Press, Beijing, China, 2011).
[15] See Supplemental Material at http://link.aps.org/supplemental/10.1103/PhysRevLett.115.227001 for the detailed solutions of the tight-binding Hamiltonian, supplemental discussions on the band structure fitting, a comparison with previous theoretical studies, the one-loop RG equations, and the Luttinger parameters away from the condition of atomic orbital rotational symmetry.
[16] J. Solyom, Adv. Phys. **28**, 201 (1979).
[17] T. Giamarchi, *Quantum Physics in One Dimension* (Oxford University Press, Oxford, UK, 2003).
[18] E. Arrigoni, Phys. Lett. A **215**, 91 (1996).
[19] H.-H. Lin, L. Balents, and M. P. A. Fisher, Phys. Rev. B **56**, 6569 (1997).
[20] Y. A. Krotov, D.-H. Lee, and S. G. Louie, Phys. Rev. Lett. **78**, 4245 (1997).
[21] J. Gonzalez and E. Perfetto, Phys. Rev. B **72**, 205406 (2005).
[22] D. Carpentier and E. Orignac, Phys. Rev. B **74**, 085409 (2006).
[23] In the Luttinger liquid approach the electronic interactions among various MO bands impact the kinetic Hamiltonian after bosonization, leading to reconstruction of the original DFT bands. So we shall use the concept "channel" for the three diagonal quasiparticle bands as defined in Eq. (7).
[24] The three-band instability discussed in Ref. [22] may appear when the electron-phonon coupling is relatively larger than the pair hopping or the Hund's coupling.
[25] C. Castellani, C. R. Natoli, and J. Ranninger, Phys. Rev. B **18**, 5001 (1978).
[26] The present study does not exclude the possibility of a spin singlet pairing due to the critical nature of the channel 3.
[27] Z. Wang *et al.*, arXiv:1502.04304v1.
[28] L. Vaugier, H. Jiang, and S. Biermann, Phys. Rev. B **86**, 165105 (2012).
[29] T. Kong, S. L. Budko, and P. C. Canfield, Phys. Rev. B **91**, 020507 (2015).